Conf-750231--1

EMISSION COMPUTERIZED-TOMOGRAPHY AND DETERMINATION OF LOCAL BRAIN FUNCTION

David E. Kuhl, M.D., Abass Alavi, M.D., Martin Reivich, M.D.

Roy Q. Edwards, Craig A. Fenton, M.D., and Robert A. Zimmerman, M.D.

From the Department of Radiology and the Department of Neurology (Dr. Reivich) of the Hospital of the University of Pennsylvania, Philadelphia, Pennsylvania.

Presented at the symposium "The Past, Present, and Future of Non-invasive Brain Imaging", Salt Lake City, Utah, 19 February, 1975 (to be published in volume of proceedings by the Society of Nuclear Medicine)

NOTICE

This report was prepared as an account of work sponsored by the United States Government. Neither the United States nor the United States Energy Research and Development Administration, nor any of their employees, nor any of their contractors, subcontractors, or their employees, makes any warranty, express or implied, or assumes any legal liability or responsibility for the accuracy, completeness or usefulness of any information, apparatus, product or process disclosed, or represents that its use would not infringe privately owned rights.

MASTER

DISTRIBUTION OF THIS DOCUMENT UNLIMITED

EMISSION COMPUTERIZED-TOMOGRAPHY AND DETERMINATION OF LOCAL BRAIN FUNCTION

David E. Kuhl, M.D., Abass Alavi, M.D., Martin Reivich, M.D.,
Roy Q. Edwards, Craig A. Fenton, M.D., and Robert A. Zimmerman, M.D.

The subject of this paper, emission computerized-tomography (CT) (1-3), is closely related as a study method to transmission CT (4-6). Both use computer reconstruction of scan data to produce transverse section pictures of the brain. The transmission CT scanner[1] uses a scanning x-ray beam to produce a cross-section picture of photon absorption differences in the brain. The emission CT scanner[2] detects gamma rays emitted from radioactive pharmaceuticals which have been administered to the patient for the purpose of brain study. A cross-section picture of brain radioactivity results. The two classes of instrument have many features in common but have the potential of producing complimentary information of quite different significance. The role of the transmission CT scanner now seems assured in the diagnosis and management of patients with a wide variety of brain disease. At the same time, the new potential for emission CT scanning is just unfolding and remains to be clarified. We suggest here that the most important contributions of transmission CT scanning are likely to be preeminent in portrayal of local brain structure while emission CT scanning seems best adapted to portrayal of local brain function.

1. For example, the EMI Scanner.

2. For example, the MARK III Scanner described in reference 7.

Pertechnetate Imaging

In delayed brain scans, the differential brain concentration of radioactive pertechnetate usually reflects the integrity of the blood brain barrier for this substance. In our earlier studies (3), we employed the emission CT scan to complement the basic four-view rectilinear study in selected patients in order to clarify the diagnosis. We concluded that the double advantage of image separation and greater sensitivity of the section method improved detection of tumors, especially those located in the basal regions of the brain, while the cross-section format gave superior description of lesion tomography such as location, boundaries, multiplicity, and shape.

While an extensive comparison of transmission CT scanning and conventional nuclide imaging is underway now in many laboratories, a careful comparison of the transmission and emission forms of CT scanning remains to be accomplished. We have only just acquired a transmission CT scanner[1] and have done very few comparison studies with our MARK III emission CT scanner (7). The corresponding complementary character of findings in these early studies are illustrated by the following cases.

The scans shown in Figures 1 and 2 are of a patient (R.M.) with lung carcinoma metastatic to the brain. The diagnosis is apparent in the conventional images made with a scintillation camera after injection of ^{99m}Tc pertechnetate (Figure 1). The initial transmission CT scan (Figure 2a) is abnormal, but the lesions are more dramatically enhanced after intravenous injection of contrast media (Figure 2b). Note the close correspondence of the emission CT scan (Figure 2c) with the transmission scan. Note the c ear separation of individual lesions in both section scans and their superiority to the vertex camera image in Figure 1.

---

1. EMI Scanner with 160 x 160 pel matrix.

The second patient (E.D.) has an intracerebral hematoma involving the region of the internal capsule, posterior limb, and the region of the posterior part of the putamen (Figure 3). The conventional nuclide images showed diffuse increase in uptake in the left posterior temporal region. The transmission CT scan dramatically defines the dense central hematoma while the corresponding emission CT scan demonstrates a "donut" sign, presumably representing increased uptake in the infarc brain immediately adjacent to the hematoma.

The next patient (G.H.) has infarction in the distribution of the right middle cerebral artery (Figure 4,5). The initial pertechnetate flow sequence is strikingly abnormal, demonstrating a prolonged transit time through the right hemisphere (Figure 4). The subsequent delayed images with the scintillation camera appeared completely normal (Figure 4). Both CT scans were abnormal. The transmissio CT scan (Figure 5) demonstrates focal reduction in attenuation in the region of the right internal capsule with extension into the frontal lobe. The emission CT scan demonstrates minimal, but definite, increased uptake of pertechnetate in a corresponding region. This case illustrates reinforcement of diagnosis by correspon pieces of data. The initial pertechnetate flow study was the most dramatically abnor finding. This case also illustrates that just as the transmission CT scan is able to distinguish attentuation differences that cannot be seen in conventional radiography, so also the emission CT scan can distinguish differences in radionuclide concentration that cannot be seen in conventional nuclide imaging.

The method requires an injection of labelled (^{99m}Tc) red cells into a peripheral vein followed by emission CT (transverse section) scanning of the brain. During the scan, a blood sample is taken and the activity in red cells and in plasma determined. Counting data from scanning are reconstructed and corrected to represent point-to-point concentration of radioactivity in a cross-section of the brain. The measured concentration of blood radioactivity is used to convert the brain activity to LCBV expressed in ml blood/100 g of brain tissue. The result is a two-dimensional map of LCBV which represents a cross-section of the brain at a known level.

In a series of four baboons, we found good agreement between the section scan results and the results from in vitro counting of brain samples; the coefficient of variation of the data was 6.7% for brain activity concentration and 8.1% for LCBV. The reproducibility of the scan method was estimated over a time period of several hours in an animal maintained in a steady state. The mean of the scan-determined LCBV values for a two cm square in the center of the brain was 3.22 ml blood/100 g with a coefficient variation of 6.5%. In a series of five baboons, the following equation was obtained for the regression plane which relates LCBV in the center of the brain to P_aCO_2 and mean arterial blood pressure (MABP).

$$LCBV = 2.88 + 0.049\ P_aCO_2 - 0.013\ MABP$$

These data agree well with the few similar results known from the literature (Table I).

Figure 7 shows the normalized regression plane A for scan-determined LCBV and the corresponding plane B for external counting data which were obtained without

TABLE I - Comparison of this and published work for alteration of LCBV in response to alteration of P_aCO_2 and MABP.

ANIMAL	P_aCO_2 Slope	MABP Slope	References
Goat	0.043		Smith et al, 1971 (15
Rhesus Monkey	0.049		Phelps et al, 1973 (1
Rhesus Monkey		-0.015	Grubb et al, 1973 (1
Baboon	0.049	-0.013	This work

benefit of section reconstruction. Note the disparity in slopes. External counting without section reconstruction is an insensitive indicator of CBV, as would be expected, since there is no discrimination against the effect on the data of extracerebral circulation.

In patients, LCBV values range from 2-4 ml/100 g depending on location, with higher values corresponding to regions of cerebral cortex. An example of an LCBV scan is shown in Figure 8.

MARK IV Scanner

Until now, the extension of emission CT scanning in this laboratory has been limited by sensitivity of our MARK III Scanner (7). This instrument has four scintillation detectors, each with a crystal that is 2" in diameter. We have now substantially completed and are testing the MARK IV transverse section imaging system which we designed to be at least ten times more sensitive than our existing MARK III instrument. This sensitivity improvement is crucial for proper extension of this study method. The device (Figure 9) includes a continuously rotating quad-octal array of 32 collimated NaI (Tl) crystal (3"-high, 1"-wide, 1"-thick), arranged eight on a side as a box about the head. As the detector square rotates, data are collected continuously, processed in the pulse height analyzers, and extracted from the rotating unit. At the same time, image reconstruction to transverse section format is accomplished with a virtual real-time processing display system. The instrument will operate initially for detection of 140 kev gamma rays (^{99m}Tc), but later an accommodation will be made for alternative use in coincidence counting of annihilation radiation from positron emitters. When applied to our studies of local brain function, this instrument should provide faster, more complete, and more accurate survey of the brain.

DISCUSSION

A clear knowledge of regional function would be of great value in the detection, localization of a wide variety of diseases and in the assessment of patient status under treatment. For instance, it has been well recognized that the treatment of a brain tumor patient requires knowledge of whether or not tumor is present and, if so, it is necessary to know as precisely as possible the location of the tumor. Also, the management of this patient would benefit from a day-to-day knowledge of the status of the blood flow, metabolism, permeability, brain swelling, and other functions on a point-to-point regional basis throughout the brain. This kind of information has not been available. Instead, function of body parts is usually examined only in the organ as a whole and regional information is usually restricted to morphology as determined by radiographic or radionuclide imaging studies. The care of patients would be enhanced if there were available non-invasive studies which would provide information of body function localized precisely within relevant body regions.

Complimentary data from different imaging modalities will always be required for adequate assessment of patients. But for assessment of regional function, radionuclide imaging is the most promising of imaging modalities. This is because of the potential here for labelling of an enormous number and variety of natural and artific compounds, chosen for a specific purpose and capable of being measured from outside the body after injection of an extremely small amount into the patient. Emission imaging potentially permits quantitative estimates of time-course of labelled compounds through structures deep within the body. This potential has only been

realized partially. One reason for present restrictions is the difficulty in isolating counting data originating from a small part of an internal organ when the differential concentration of radionuclide is small between the organ and its surrounding and the structure of interest is deep within the body.

As a general method, three-dimensional reconstruction of radionuclide scan data should become more important in the study of the brain. Ideally, such a technique should enable precise measurement of radionuclide concentration to be determined within functional structural units of the brain in man which has not been possible up until now. The same study principles might be applied to other tracers enabling measurements of local cerebral blood flow and local metabolic rates for various metabolitics within the brain in man. Measuring these kinds of regional function, with three-dimensional resolution throughout the brain and without the necessity for intra-carotid injection of indicator, could become a significant advance over the presently available methods.

ACKNOWLEDGEMENT

This investigation was supported in part by USPHS Research Grant 2R01 GM-16248, USAEC Contract AT(11-1)-3399, USPHS Program Project Grant 5P01NS-10930, and USPHS Research Career Development Award 2-KS-HS-11 (Dr.M.R). USAEC # COO-3399-6.

REFERENCES

1. Kuhl, D.E., and Edwards, R.Q. Image Separation Radioisotope Scanning. Radiology 80: 653-662, April 1963.

2. Kuhl, D.E., Pitts, F.W., Sanders, T.P., and Mishkin, M.M.: Transverse Section and Rectilinear Brain Scanning Using ^{99m}Tc Pertechnetate, Radiology 86: 822-829, May, 1966.

3. Kuhl, D.E., and Sanders, T.P.: Characterizing Brain Lesions Using Transverse Section Scanning. Radiology 98: 317-328, Feb, 1971.

4. Kuhl, D.E., Hale, J., and Eaton, W.L.: Transmission Scanning: A Useful Adjunct to Conventional Emission Scanning for Accurately Keying Isotope Deposition to Radiographic Anatomy. Radiology 87: 278-284, Aug 1966.

5. Hounsfield, G.N.: Computerized Transverse Axial Scanning (Tomography): Part 1. Description of System. British Journal of Radiology 46: 1016-1022, Dec 1973.

6. Ambrose, J.: Computerized Transverse Axial Scanning (Tomography): Part 2: Clinical Application. British Journal of Radiology. 46: 1023-1047, Dec 1973.

7. Kuhl, D.E. and Edwards, R.Q.: The MARK III Scanner: A Compact Device for Multiple-View and Section Scanning of the Brain. Radiology 96: 563-570, Sept 1970.

REFERENCES

8. Kuhl, D.E., Edwards, R.Q., Ricci, A.R., and Reivich, M.: Quantitative Cross Section Scanning Using Orthogonal Tangent Correction. J. Nucl Med 12: 193-208, April, 1971.

9. Edwards, R.Q. Ricci, A.R., Kuhl, D.E.: Cumulative Additive Tangent Correction (CATC): An Improved Technique for Three-Dimensional Reconstruction of Radionuclide Scan Data (In Press).

10. Ter-Pogossian, M.M., Phelps, M.E., Hoffman, E.J., and Mullani, N.A.: A Positron-Emission Transaxial Tomograph for Nuclear Imaging (PETT). Radiology 114: 89-98, Jan 1975.

11. Budinger, T.F., and Gullberg, T.T.: Three-Dimensional Reconstruction In Nuclear Medicine By Iterative Least-Squares and Fourier Transform Techniques. USAEC Report LBL-2146, TID-4500-R61, Jan 1974.

12. Kuhl, D.E., Reivich, M., Alavi, A., Nyary, I., and Staum, M.M.: Local Cerebral Blood Volume Determined by Three-Dimensional Reconstruction of Radionuclide Scan Data, (In Press).

13. Risberg, J. and Ingvar, D.H.: Regional Changes in Cerebral Blood Volume during Mental Activity. Exp. Brain Research 5: 72-78, 1963.

14. [illegible], J., [illegible], and Ingvar, D.H.: Regional Cerebral Blood Volume during Paradoxical Sleep. In: [illegible], M., Fieschi, C., Ingvar, D.H., [illegible], M.A., and [illegible], K. [illegible]. [illegible] Blood Flow. Clinical and Experimental Results. Springer, Berlin, pages 101-103, 1969.

15. Smith, A.L., Neufeld, J.R., Ominsky, A.J., and Wollman, H: Effect of Arterial CO_2 Tension of Cerebral Blood Flow, Mean Transit Time, and Vascular Volume, J. Appl. Physiol. 31: 701-707, 1971.

16. Langfitt, T.W., Weinstein, J.D., and Hassell, N.F.: Cerebral Vasomotor Paralysis Produced by Intracranial Hypertension. Neurology 15:662-643, 1965.

17. Oldendorf, W.H. and Lisaka, Y.: Interference of Scalp and Skull with External Measurements of Brain Isotope Content: Part I Isotope Content of Scalp and Skull. J. Nuc. Med 10: 177-183, 1969.

18. Phelps, M.E., Grubb, R.L., and Ter-Pogossian, M.M: Correlation Between $PaCO_2$ and Regional Cerebral Blood Volume by X-ray Fluorescence. J. Appl. Physiol 35: 274-280, Aug 1973.

19. Grubb, R.L., Jr., Phelps, M.E., Raichle, M.E., and Ter-Pogossian, M.M.: The Effects of Arterial Blood Pressure on the Regional Cerebral Blood Volume by X-ray Fluorescence. Stroke, 4: 390-399, 1973.

LEGENDS

Figure 1 Patient (R.M.). Brain metastases. Conventional images made with a scintillation camera after injection of ^{99m}Tc pertechnetate clearly demonstrate multiple spherical regions of increased uptake.

Figure 2 Patient (R.M.) with brain metastases shown in Figure 1. The initial transmission CT scan (A) is abnormal, but the lesions are delineated better after intravenous injection of contrast media (B). The emission CT scan (C) corresponds closely to transmission scan B. Note the clear separation of individual lesions in both section scans and their superiority over the vertex camera image in Figure 1.

Figure 3 Patient (E.D). Intracerebral hematoma. The conventional ^{99m}Tc pertechnetate images made with scintillation camera (A,B) show diffuse increased uptake in the left posterior temporal region. The transmission CT scan (C) defines the dense central hematoma while the corresponding emission CT scan (D) demonstrates a "donut" sign, presumably representing increased uptake of radioactivity in the infarcted brain immediately adjacent to the hematoma.

LEGENDS

Figure 4 Patient (G.H.). Infarction in distribution of right middle cerebral artery. The initial ^{99m}Tc pertechnetate flow sequence is strikingly abnormal; there is a prolonged transit time through the right hemisphere (top). The subsequent delayed images with the scintillation camera appear completely normal (bottom).

Figure 5 Patient (G.H.). Infarction in distribution of right middle cerebral artery. The transmission CT scan (A) demonstrates focal reduced attenuation in the region of the right internal capsule with extension into the frontal lobe. The corresponding emission CT scan (B,C) shows increased uptake of radioactivity in the same region, even though the conventional nuclide scans were normal.

Figure 6 Accuracy of predicting relative concentration by tangent correction reconstruction of emission CT scan data. (CATC process, reference 9)

(A) Bottle Phantom. Each bottle measures 3 cm x 3 cm in section plane. Relative concentrations of ^{99m}Tc are marked on bottle tops.

(B) Processed scan after application of attenuation correction mask. Total 1.5 million counts.

(C) Relative concentrations from scan data agree with real values with a coefficient of variation of 5.6%.

LEGENDS

Figure 7 Response of CBV to P_aCO_2 and MABP. The slopes are different for the two normalized regression planes (plane A=external counting data with section reconstruction and plane B=external counting data without section reconstruction). The base slope of plane B is opposite in sign to what would be expected with autoregulation. External counting without section reconstruction is an insensitive indicator of CBV.

Figure 8 (G.D) Section scans of a malignant glioma which is surrounded by edema. A^T the tope of the figure, section scans of ^{99m}Tc pertechnetate show the alteration of blood brain barrier. At the bottom , section scans of ^{99m}Tc red cells show local cerebral blood volume. Initial studies are to the left in the figure and studies made two months later, after steroid therapy, are to the right. The section scans of ^{99m}Tc red cells show a large region of reduced LCBV due to compression of local microcirculation by edema. After steroid therapy, peritumor edema decreases and peritumor LCBV returns toward normal.

LEGENDS

Figure 9 The HAWK IV transverse section imaging system now in final stages of construction. For high sensitivity, the instrument has 32 collimated detectors arranged eight on a side as a box about the head. The detector square rotates continuously. At the same time, data are reconstructed to section format with a virtual real-time processing display system.

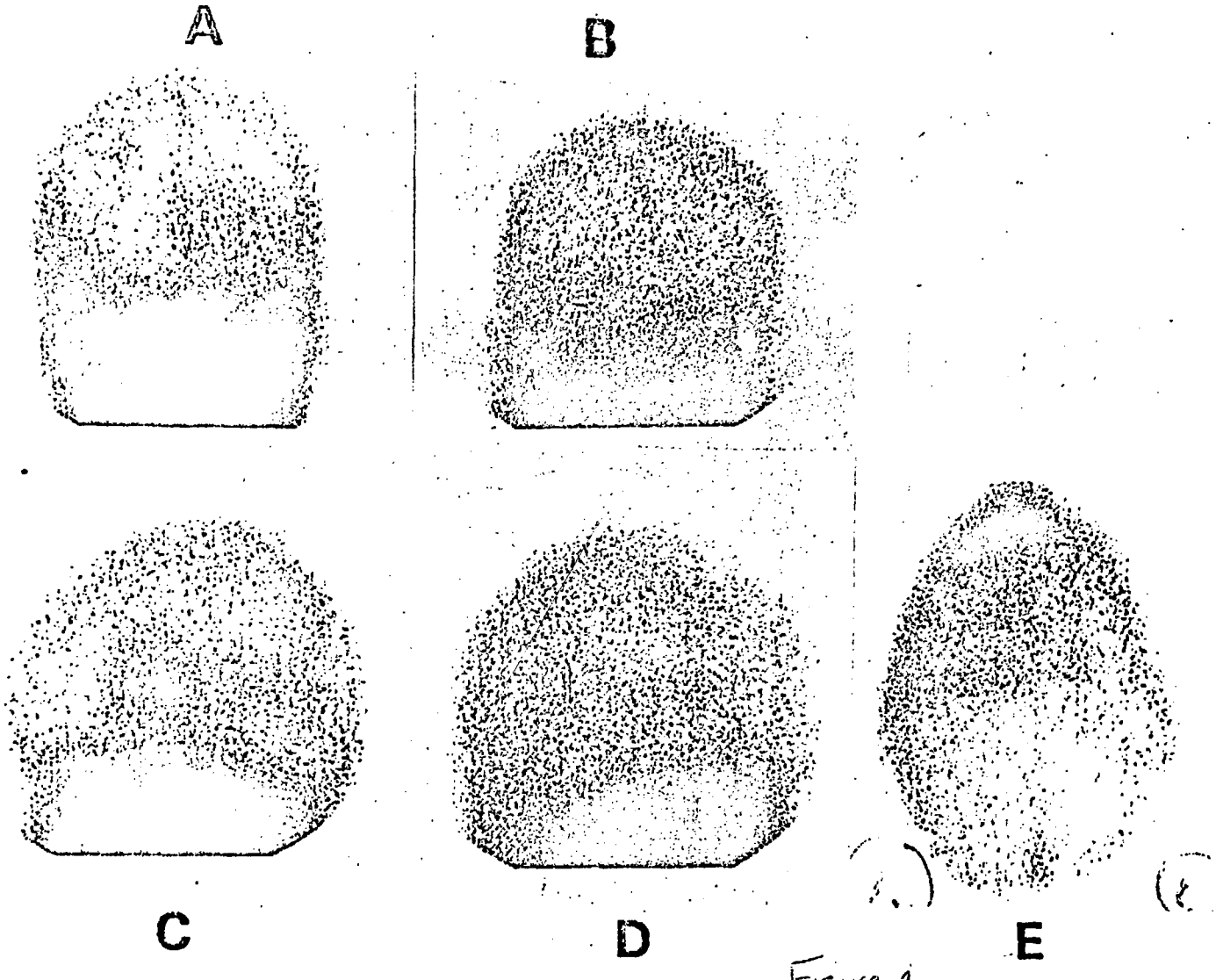

Figure 1

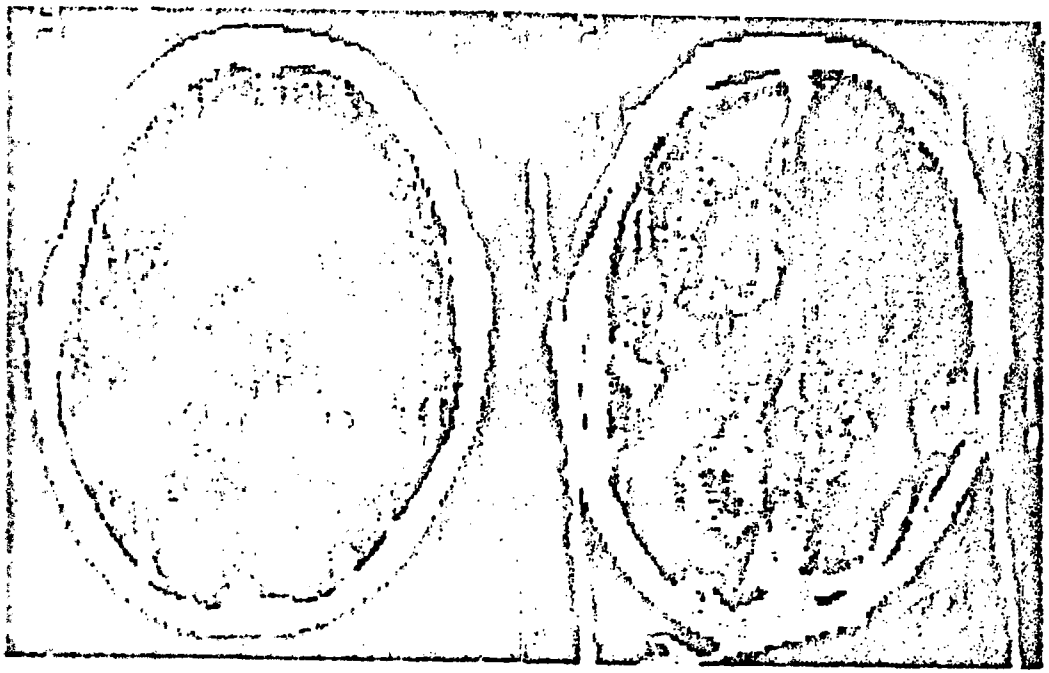

A B

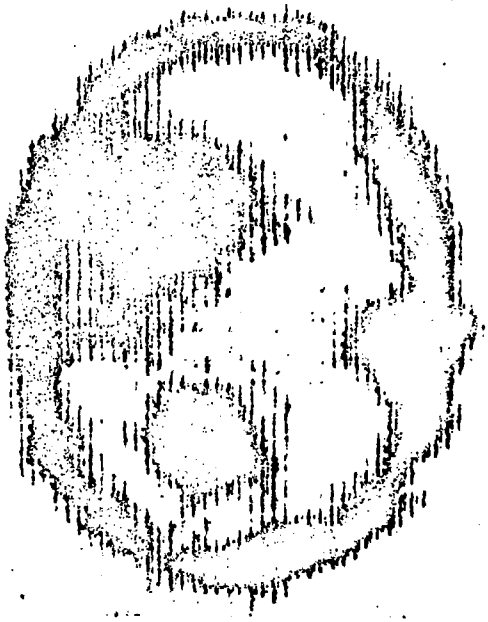

C

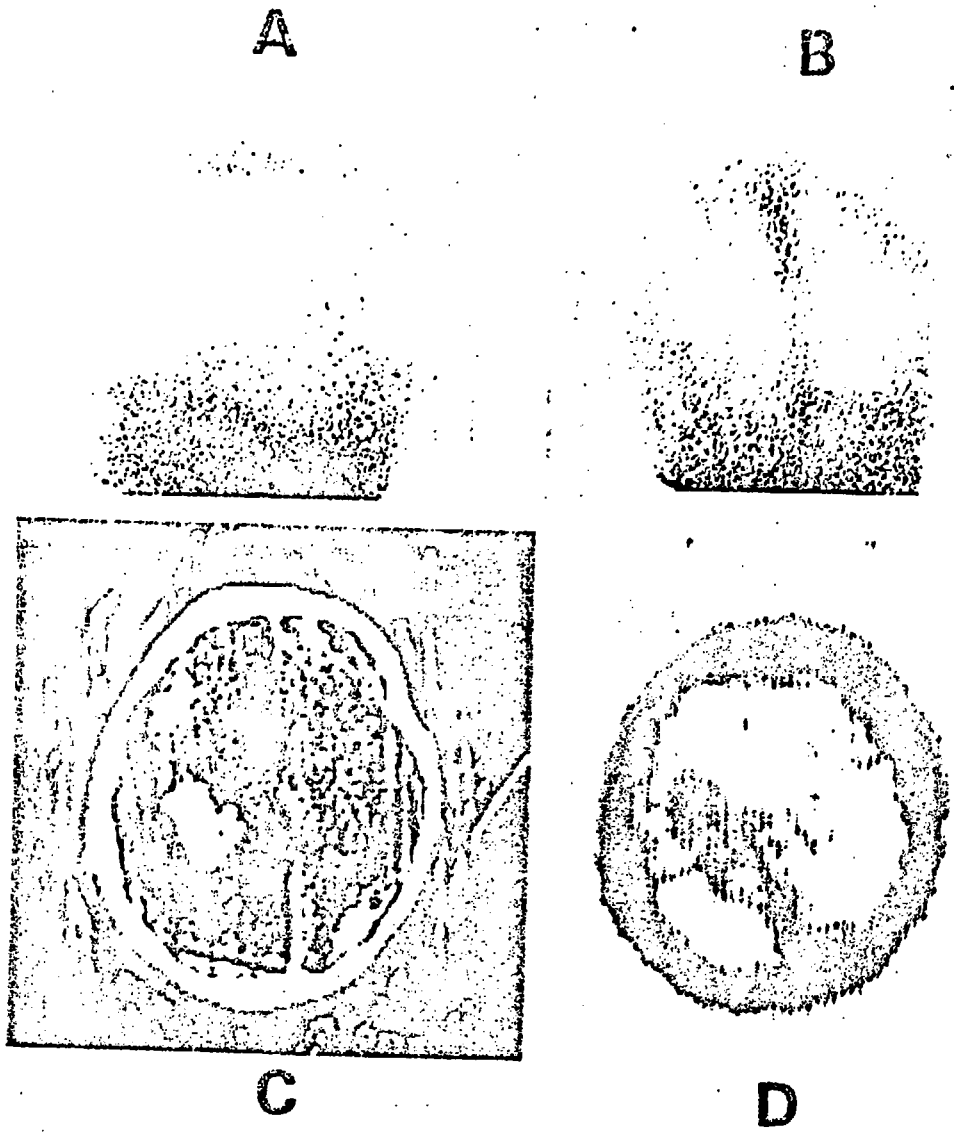

Figure 3

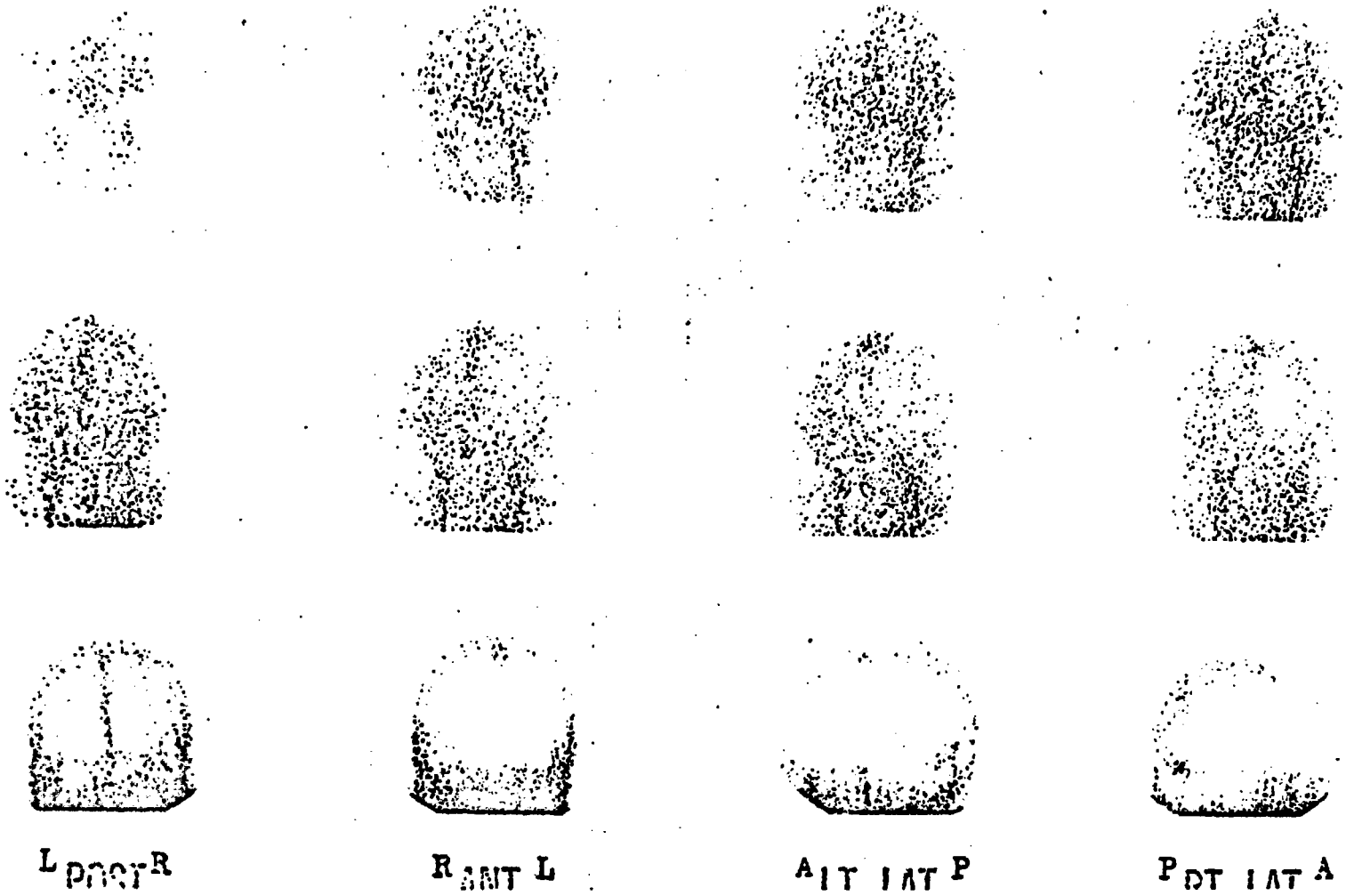
L POST R
R ANT L
A LAT P
P DT LAT A

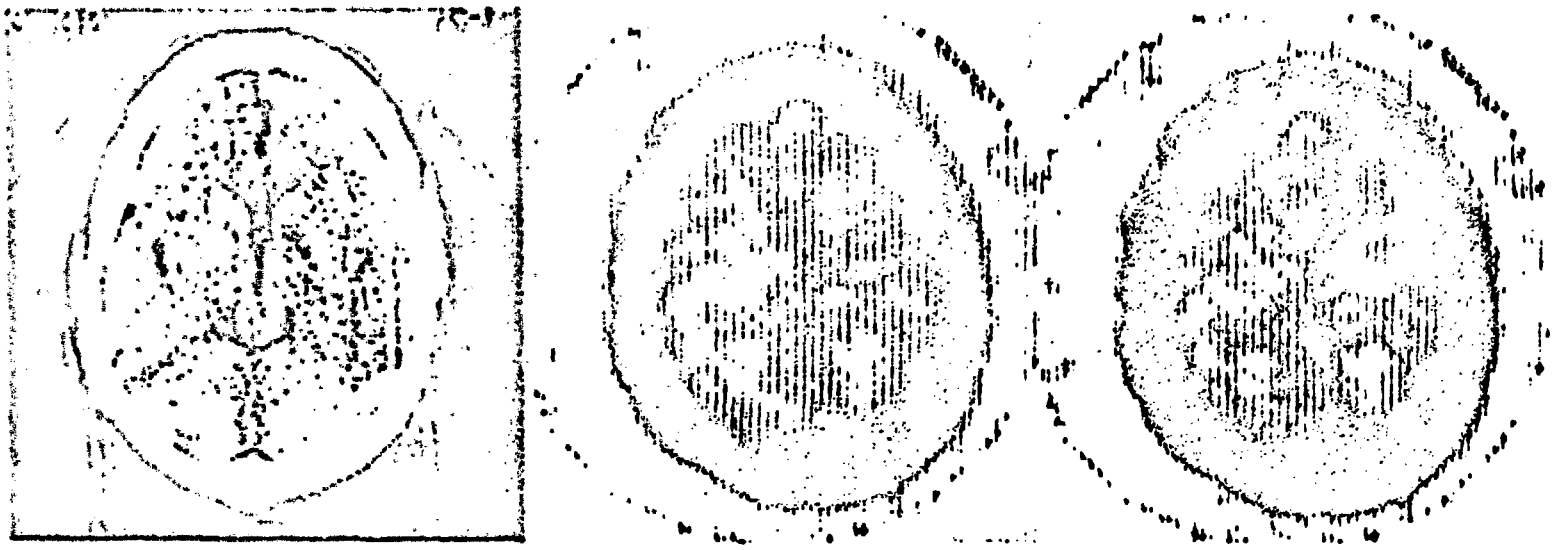

A B C

Figure 5

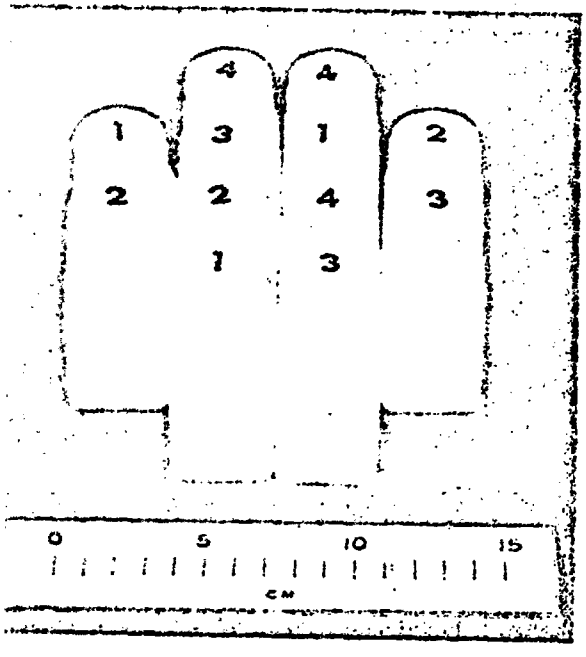

	4.15	4.01	
0.97	3.16	1.13	1.97
2.02	2.05	3.79	2.86
	1.07	2.82	

Figure 6

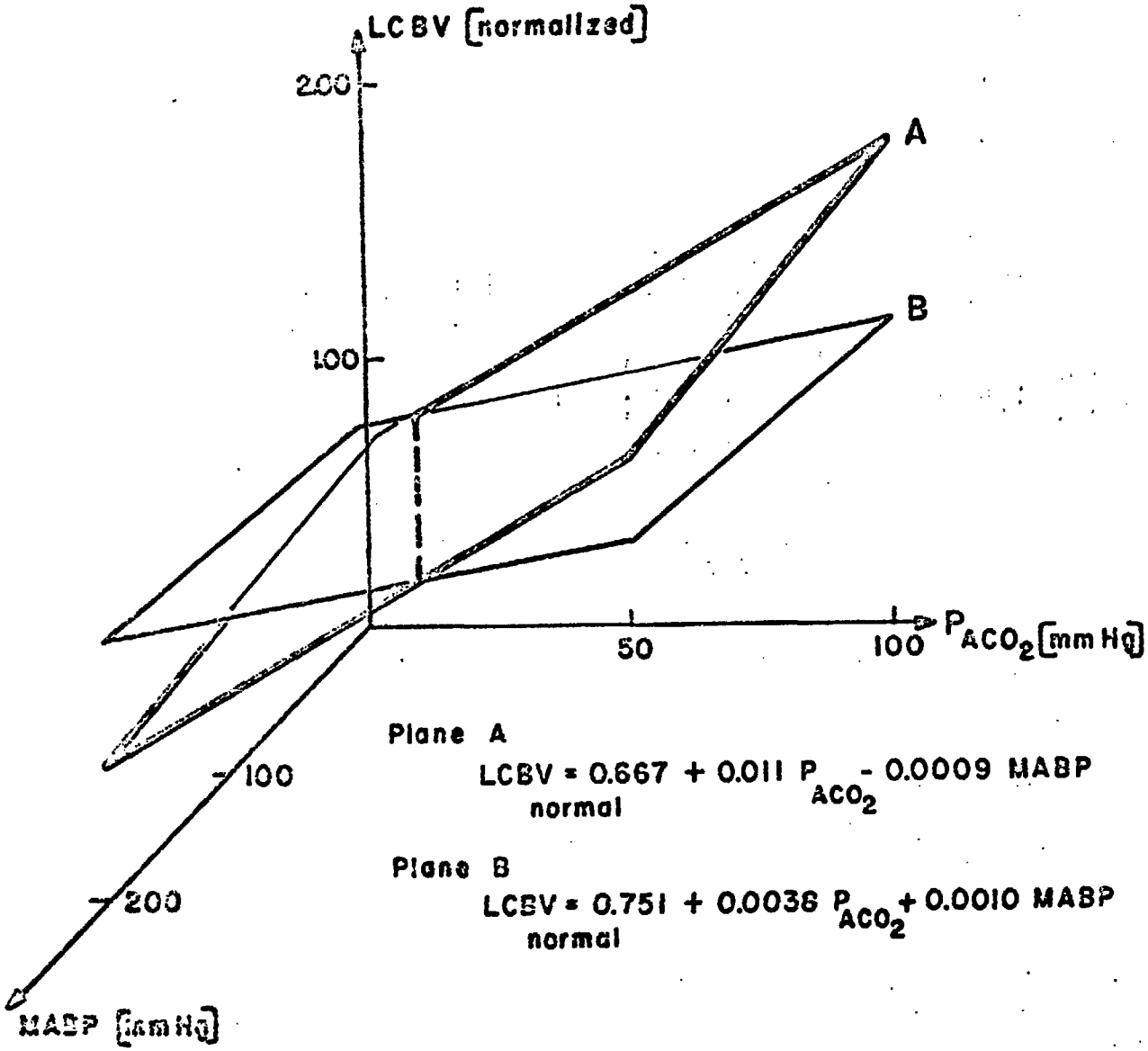
LCBV [normalized]
200
100
A
B
50
100
P_{ACO_2} [mm Hg]
100
200
MABP [mm Hg]
Plane A
$LCBV_{normal} = 0.667 + 0.011\ P_{ACO_2} - 0.0009\ MABP$
Plane B
$LCBV_{normal} = 0.751 + 0.0038\ P_{ACO_2} + 0.0010\ MABP$

Figure 7

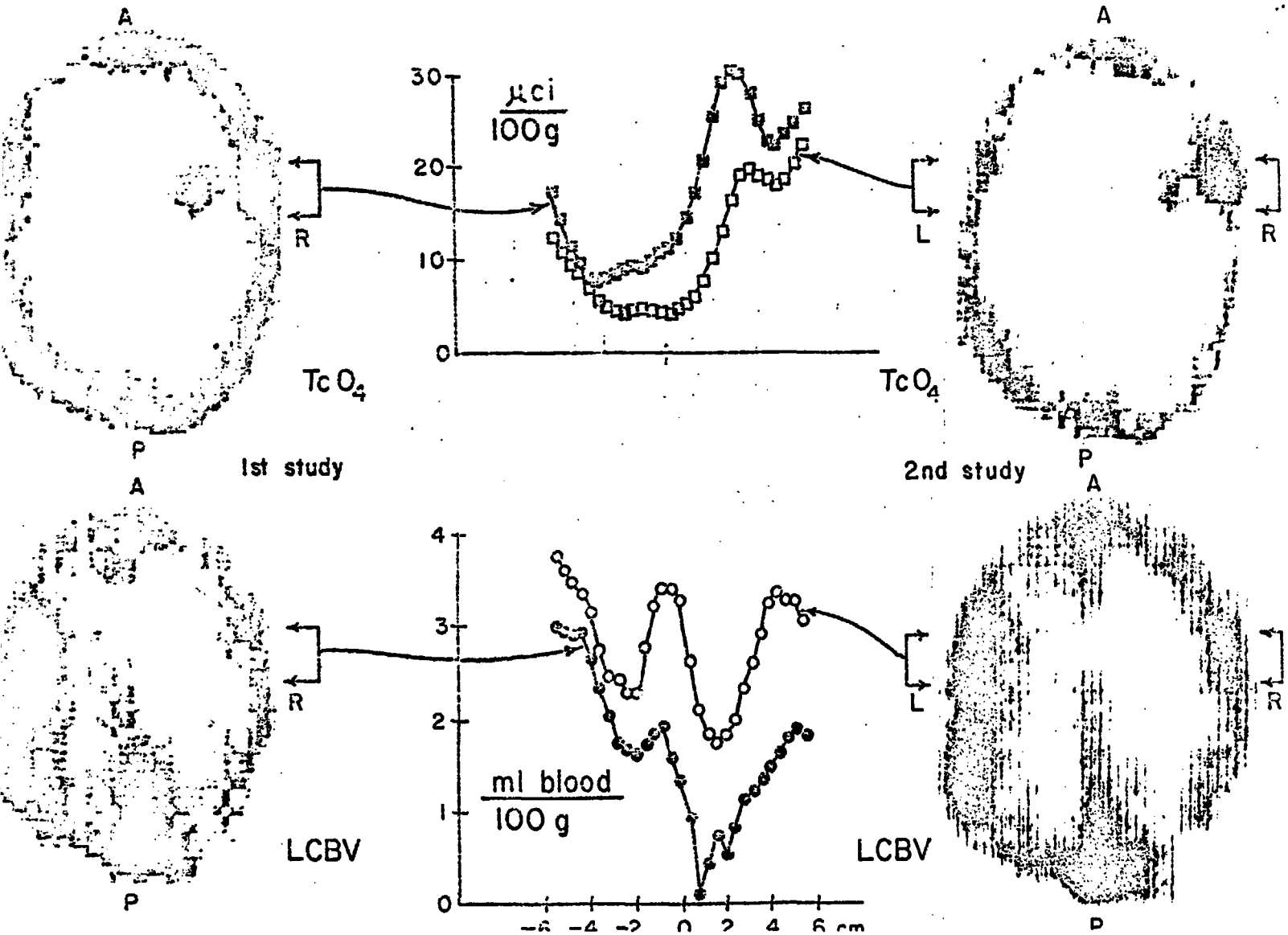
A
R
P
TcO4
1st study
30
20
10
0
μci
100g
L
TcO4
A
R
P
2nd study
A
R
P
LCBV
4
3
2
1
0
ml blood
100 g
-6 -4 -2 0 2 4 6 cm
L
LCBV
A
R
P

Figure 8

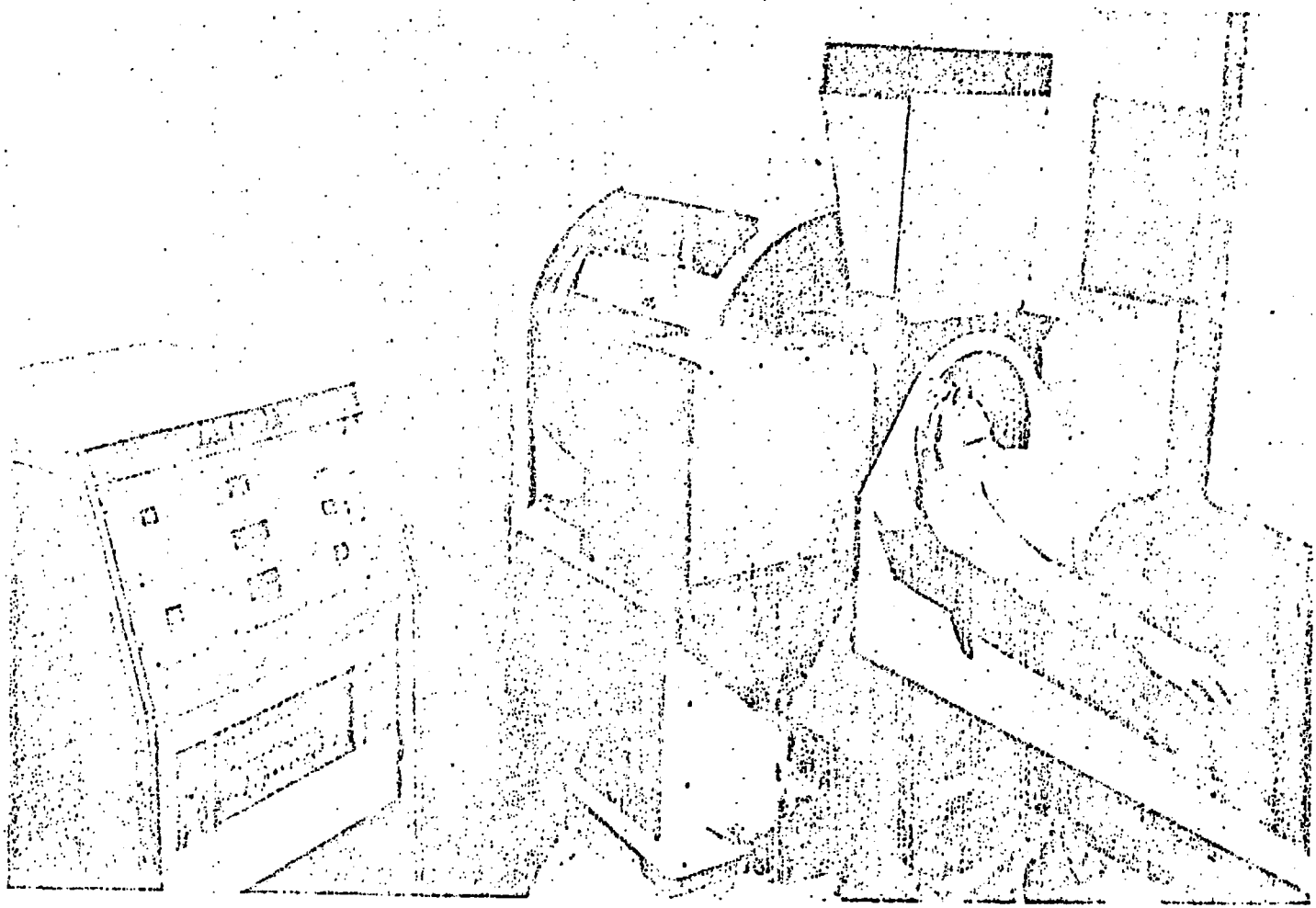

Figure 9